Multichannel Conical Emission and Parametric and Nonparametric Nonlinear Optical Processes in Ytterbium Vapor

B. DeBoo[a], D.F. Kimball[a], C.-H. Li[a], and D. Budker[a,b,*]

[a]Department of Physics, University of California at Berkeley,

Berkeley, CA 94720-7300

[b] Nuclear Science Division, Lawrence Berkeley National

Laboratory, Berkeley CA 94720

[*] *budker@socrates.berkeley.edu*

Collimated and conical emissions that appear when ytterbium vapor is illuminated by light pulses at 262 nm (near the one-photon Yb $6s^2\ {}^1S_0 \rightarrow 6s7p\ {}^3P_1$ transition) are experimentally investigated. Conical emission is observed at multiple wavelengths. Parametric and nonparametric nonlinear optical processes are studied by investigating the spatial distribution of generated light and the efficiency of light generation as a function of incident light frequency.

OCIS codes: 190.2620, 190.4180, 190.4380, 190.4410

1. Introduction

A variety of nonlinear optical effects can be observed when intense, near-resonant light propagates through a dense atomic medium [1, 2, 3, 4, 5]. For example, when laser light tuned near a one-photon transition interacts with a multilevel atomic system, emissions can be generated at frequencies different from that of the incident light (see, e.g., Refs. [6, 7, 8] and references therein). Under certain conditions, the generated light can be emitted in hollow cones [6, 8, 9, 10, 11, 12, 13, 14, 15, 16]. Such conical emission (CE) has been observed at wavelengths near that of the incident laser light (see, e.g., [13, 14, 15, 16, 17] and references therein) and also at wavelengths corresponding to other atomic transitions [9, 10, 11, 12]. Collimated light (light emitted in a filled-in cone with relatively small angle of divergence compared to CE) can be generated in both the forward and backward directions with respect to the propagation direction of incident laser light (see, e.g., [1] and references therein). The nonlinear generation can be attributed to a combination of several processes such as stimulated Raman scattering (SRS) and amplified spontaneous emission (ASE) (both nonparametric), as well as parametric four-wave mixing (4WM).

There is considerable interest in understanding the role of different physical mechanisms in nonlinear generation of light, e.g., for the development of new ultraviolet lasers (see, e.g., Ref. [18]). In this experiment, we observe radiation generated in a dense ytterbium vapor by light pulses at 262 nm (near the one-photon $6s^2\ {}^1S_0 \rightarrow 6s7p\ {}^3P_1$ transition) via both parametric and nonparametric processes. We measure spatial profiles of emission at different wavelengths and total emission energies as a function of incident light frequency and observe distinct behavior for light generated by parametric and nonparametric processes. Several features of this experiment, such as observation of CE near-resonant with transitions between excited atomic states, distinguish it from previous, closely-related work in sodium vapor employing one-photon excitation [6, 8, 9, 10, 11, 12, 13]. The nonparametric nonlinear processes investigated in this work may be useful in a new

scheme to measure atomic parity nonconservation (PNC) in Yb [19]. In this scheme, one would search for PNC-induced optical rotation on the 1.28 μm 6s6p ^{3}P$_0$ $\rightarrow$ 6s6p ^{1}P$_1$ transition. Nonlinear processes may allow relatively fast and efficient population of the 6s6p ^{3}P$_0$ metastable state for such an experiment.

2. Experimental Setup

The experimental apparatus (various details of which have been described elsewhere [20, 21]) is shown in Fig. 1. Several grams of Yb metal with natural isotopic abundance are placed in the center of a resistively-heated, tantalum-lined stainless steel vapor cell. In these experiments, the cell contains neon buffer gas at pressures of 1 - 15 Torr (measured with a capacitance manometer). The central region of the vapor cell is heated to $\approx$ 1150 K, as measured by a thermocouple placed at the middle of the cell. The ends of the vapor cell, fitted with optical windows, are water cooled; Yb vapor condenses before it reaches the windows. The column length of the vapor (estimated from the distance between regions where Yb condenses) is $\sim$ 30 cm, and the average Yb density is $\sim$ 10^{17} atoms/cm^3. The density is estimated from the Yb saturated vapor pressure [22] at this cell temperature.

The pulsed 262 nm beam is produced by an excimer- (Lambda Physik EMG 101 MSC) pumped dye laser (Lambda Physik FL 2002) with frequency doubling. The laser system operates with a repetition rate of 5 Hz and 262 nm pulses, which propagate along the axis of the vapor cell, have a duration of $\approx$ 20 ns, spectral width of $\sim$ 20 GHz (according to the Lambda Physik FL 2002 specifications), an energy of $\approx$ 0.4 mJ, and an area of $\sim$ 0.02 cm^2 with roughly circular cross section. Various measurement devices specific to each experiment (optical fiber directing light into a spectrometer, photodiodes with interference filters, a CCD camera, etc.) were placed in front or back of the vapor cell, as discussed below. A dichroic mirror which directs the 262 nm light into

the vapor cell allows observation of visible light generated in the backward direction.

3. Experimental Observations and Discussion

In order to determine the wavelengths of generated light, emissions from the vapor cell in the forward and backward directions (with respect to the propagation direction of 262 nm light) were focused into a multimode fiberoptic cable. The output of the cable was directed into a grating spectrometer (Jarrell-Ash Czerny-Turner Model II), which has a resolution of $\sim$0.01 nm. The spectrometer grating was scanned through the entire visible and near-IR wavelength range and the emission intensity at different wavelengths was measured with an EMI 9658 prismatic phototube installed at the output slit of the spectrometer. In order to distinguish between first order and higher order ("ghost") reflections from the spectrometer grating, various combinations of color glass and interference filters were placed between the output of the fiberoptic cable and the input slit of the spectrometer. From these measurements, we determined that there were four prominent emission lines in the wavelength range studied: 556 nm, 611 nm, 649 nm, and 680 nm. Emissions at 649 nm and 680 nm were observed in both forward and backward directions, while 556 nm and 611 nm emissions were observed only in the forward direction. The spectral width of the emissions was $\sim$ 20 GHz, similar to the specified spectral width of the incident 262 nm light. The resolution of the spectrometer was insufficient to resolve any detailed spectral characteristics of the emissions. There were also relatively intense infrared (IR) emissions (beyond the spectrometer scan range) which were observed directly with a PbS detector fitted with IR filters. Unfortunately, the PbS detector was inadequate for detailed measurements of the intensity or spatial distribution of IR emissions.

The intensities and durations of emissions clearly indicate that the light is generated by non-linear processes, rather than ordinary fluorescence. From the measured total energy of light emitted at wavelengths other than 262 nm, we estimate that when the incident light is resonant with the

$6s^2\ {}^1S_0 \rightarrow 6s7p\ {}^3P_1$ transition, ∼20% of the ultraviolet light energy is converted into collimated and conical nonlinear emissions at other wavelengths. The time duration of the emissions (∼ 20 ns, measured with a fast photodiode, FND-100) is considerably shorter than relevant natural lifetimes of atomic states (for example, the $6s7p\ {}^3P_1$ state has a lifetime of 120(30) ns [23]).

The emitted wavelengths observed are near-resonant with various atomic transitions in Yb (Fig. 2). The 649 nm emission corresponds to a transition ($6s7s\ {}^3S_1 \rightarrow 6s6p\ {}^3P_0$) to a metastable state. Since 649 nm emission cannot be generated by parametric processes (in which the initial and final states of the atomic system are identical [3]) it is said to occur along a "nonparametric channel." Emissions at 611 nm ($6s7s\ {}^1S_0 \rightarrow 6s6p\ {}^3P_1$), 680 nm ($6s7s\ {}^3S_1 \rightarrow 6s6p\ {}^3P_1$), and 556 nm ($6s6p\ {}^3P_1 \rightarrow 6s^2\ {}^1S_0$) are near-resonant with transitions along cascades connecting to the ground state. These wavelengths, which can be generated by parametric amplification, are said to occur along "parametric channels" (note, however, that light produced along a parametric channel is *not precluded* from being produced by nonparametric effects). By comparing the properties of the observed emissions under various experimental conditions, the behavior of nonparametric and parametric channels can be studied. A number of previous investigations have observed competition between parametric and nonparametric processes, in particular the suppression of ASE by 4WM processes (see, e.g., Refs. [24, 25, 26, 27, 28] and references therein), when sufficiently intense light near-resonant with a 2-photon transition propagates through a relatively dense metal vapor. Presumably, similar effects are present in the case of a one-photon transition.

The spatial intensity profiles in the forward direction were measured by focusing the emitted light into the aperture of a CCD camera (Coherent LaserCam^{TM}). Images were recorded and analyzed using Beamview^{TM} beam profiling software. Appropriate neutral density and interference filters were placed between the vapor cell and the CCD camera to select the emission of interest and to reduce saturation of the detector. Light generated at 649 nm (along a nonparametric channel),

was emitted as a collimated beam (Fig. 3). For light near-resonant with transitions between excited states in a parametric channel (i.e. 680 nm, 611 nm), both CE and collimated emission are observed (Figs. 4 and 5). 556 nm light is emitted in cones with no collimated emission (Fig. 6). Typical values of the cone half angles (θ), determined by cone diameter measurements at two different distances from the end of the vapor cell, are: $\theta_{556} = 1.3^\circ \pm 0.5^\circ$, $\theta_{611} = 2.0^\circ \pm 0.5^\circ$, and $\theta_{680} = 2.6^\circ \pm 0.5^\circ$. The cone angles are relatively insensitive to 262 nm light detuning (variations $< 10\%$ over the 262 nm tuning range where nonlinear emissions were observed). A summary of the properties of the observed emissions is given in Table I.

Conical emission in multilevel systems has been commonly interpreted to be a result of photon momentum conservation (phase-matching) in parametric 4WM (see, e.g., Refs. [9, 10, 12]). Parametric processes like 4WM require that created photons have the same total energy and total momentum as the incident photon:

$$\omega_L = \omega_{IR} + \omega_R + \omega_G, \tag{1}$$

$$\vec{k}_L = \vec{k}_{IR} + \vec{k}_R + \vec{k}_G, \tag{2}$$

where ω and $\vec{k}$ are the angular frequencies and wave vectors, respectively. The subscript L refers to the incident laser light, while IR, R, and G refer to the parametrically generated light (in our case occurring at infrared, red, and green wavelengths, Fig. 2). As the phase matching picture of Fig. 7 illustrates, if one generated frequency occurs off-axis from the incident laser light then at least one other must do so as well. This behavior was predicted for CE in Na [9], but emission for wavelengths corresponding to transitions between excited states has not been observed (see Refs. [9, 10]). In Yb, CE is seen for all visible wavelengths corresponding to transitions along the parametric channels shown in Fig. 2. Light generated at 649 nm cannot be produced by a parametric process, and therefore does not exhibit CE. Similarly, emission of 680 nm in the backward direction does not exhibit CE because it must be created nonparametrically; momentum conservation in parametric 4WM

(Eq. (2), Fig. 7) requires that, under our experimental conditions [29], the generated wavelengths propagate in the forward direction.

The absence of collimated emission for the 556 nm light may be related to the fact that nonparametric processes, responsible for the collimated emission, require population inversion over the sample length (see, e.g., [2]). For the estimated number of Yb atoms in the beam path ($\sim 10^{17}$ atoms) and number of incident 262 nm photons ($\sim 7 \times 10^{14}$ photons per pulse) in this experiment, it is impossible to produce population inversion for the 556 nm 6s6p $^3P_1 \rightarrow 6s^2\ ^1S_0$ transition. Therefore, the observed 556 nm light, produced solely by parametric amplification, is not resonant with the 6s6p $^3P_1 \rightarrow 6s^2\ ^1S_0$ transition, and thus must be emitted off-axis due to the requirement of phase matching in 4WM. The fact that 556 nm emission is off-resonant is confirmed by the observation that when emitted light at 556 nm is retro-reflected through the vapor cell it is not absorbed.

To investigate the nonlinear optical processes as a function of incident light detuning, the frequency of the 262 nm light was scanned with a motor controlling the tilt angle of the dye laser oscillator diffraction grating. The frequency was determined from the laser grating position read-out. The intensity of the generated light was measured with a fast photodiode (FND-100). It was observed that 680 nm (in the backward direction) and 649 nm emissions acquire their peak intensity when incident 262 nm is on resonance (Fig. 8). The resonance in 649 nm emission in the forward direction (relative to 262 nm beam propagation) as a function of 262 nm detuning has a full-width at half-maximum ($\Delta_{649}^{(F)}$) of $\approx$20 GHz, comparable to the laser linewidth. The resonances in 649 nm and 680 nm emission in the backward direction have similar widths, $\Delta_{649}^{(F)} \sim \Delta_{649}^{(B)} \sim \Delta_{680}^{(B)}$, and are peaked where 262 nm light is resonant with the $6s^2\ ^1S_0 \rightarrow 6s7p\ ^3P_1$ transition. This indicates that emissions produced purely by nonparametric processes (649 nm light and backward emission of 680 nm cannot be created by parametric 4WM) are strongest when the 262 nm light is on resonance. On

the other hand, 680 nm emission in the forward direction, which can be produced via parametric 4WM, exhibits significant intensity even when 262 nm light is detuned from resonance: $\Delta_{680}^{(F)}$ is almost three times larger than $\Delta_{649}^{(F)}$, $\Delta_{649}^{(B)}$, and $\Delta_{680}^{(B)}$.

Fig. 9 shows the intensity of emissions in the forward direction as a function of 262 nm light detuning. For these measurements, the total pulse energy was determined by integrating over the image area of the CCD camera aperture. In addition to 649 nm and 680 nm emissions, relatively intense 556 nm and 611 nm emissions are also observed. In contrast to the behavior of 649 nm and 680 nm light, these emissions experience a dip in intensity near where 649 nm and 680 nm light acquire peak intensity (Fig. 9).

The dips in 611 nm and 556 nm intensities (when 262 nm light is on resonance) may be attributed to an interplay between parametric and nonparametric processes. When 262 nm light is on resonance, the increase in the amplitude of nonparametric processes (including resonant absorption of 262 nm) is accompanied by a corresponding decrease in parametric amplification, since the 262 nm beam is depleted as it propagates through the medium. The production of light by nonparametric processes is clearly enhanced when incident 262 nm light is on resonance, as evidenced by the peaked intensity of 649 nm light (Figs. 8 and 9). As discussed above, 556 nm light cannot be generated via nonparametric nonlinear optical processes (e.g., ASE), since it is impossible to create population inversion between the 6s6p $^3P_1$ state and the ground state under our experimental conditions. Hence, with incident 262 nm light on resonance, the interplay between parametric and nonparametric processes produces the dip in 556 nm intensity (Fig 9). In addition, experimental evidence suggests that the amplitude for nonparametric generation of light along the 611 nm channel is much smaller than that for the 680 nm channel. For example, 611 nm light (unlike 680 nm) is not observed in the backward direction. Also, in contrast to conical and forward-directed collimated emissions at 680 nm, which have similar intensities (Fig. 4), collimated emission at 611

nm is much less intense than 611 nm CE (Fig. 5). Thus, when incident 262 nm light is resonant, there is also a dip in 611 nm intensity (Fig. 9).

4. Application to the Study of Parity Nonconservation in Ytterbium

Ytterbium has been identified as a promising system with which to study atomic parity nonconservation (PNC) caused by neutral weak interactions [30] (for reviews of atomic PNC see Refs. [31, 32]). Ytterbium has a pair of closely-lying (separated by $\approx$589 cm^{-1}) opposite parity states (6s5d ^{3}D$_1$, 6s6p ^{1}P$_1$) which are strongly mixed by weak neutral current interactions. An experiment is currently in progress in this laboratory to measure PNC effects in Yb using the Stark-PNC interference technique with the 408 nm 6s^2 ^{1}S$_0$ $\rightarrow$ 6s5d ^{3}D$_1$ transition [33, 34].

Recently, an alternative scheme for measuring PNC effects in Yb that could, in principle, take advantage of the nonlinear optical effects, has been proposed [19]. The proposed experiment would measure PNC-induced optical rotation (see, e.g., Ref. [35] for a discussion of the basic principles of PNC-induced optical rotation experiments) on the 1.28 μm 6s6p ^{3}P$_0$ $\rightarrow$ 6s6p ^{1}P$_1$ transition (Fig. 10). Efficient population of the lower state of the transition (the metastable 6s6p ^{3}P$_0$ state) is crucial for such an experiment, and may be possible via the nonlinear processes discussed above when the 262 nm light is tuned to resonance. This technique may be convenient since only a single laser beam is required, as opposed to other population schemes involving two-stage excitation. This PNC scheme is discussed in more detail in Ref. [19].

5. Conclusions

Nonlinear generation of light and conical emission at multiple wavelengths have been observed in a dense Yb vapor illuminated by light near-resonant with the one photon 262 nm 6s^2 ^{1}S$_0$ $\rightarrow$ 6s7p ^{3}P$_1$ transition. Conical emission is attributed to parametric four-wave mixing, and collimated emission observed in the forward and backward directions is attributed to nonparametric processes (e.g.,

amplified spontaneous emission). The dependence of emission intensity on 262 nm light detuning can be explained based on the interplay between various parametric and nonparametric processes. The nonlinear optical effects studied may be applied in a measurement of parity nonconserving optical rotation on the Yb 1.28 μm 6s6p $^3P_0 \rightarrow$ 6s6p $^1P_1$ transition, where nonparametric processes can be used for fast and efficient population of the 6s6p $^3P_0$ state.

6. Acknowledgments

The authors would like to thank A.-T. Nguyen and S. M. Rochester for their significant contributions to various stages of the experiments, D. Clyde for crucial preliminary work, D. DeMille and M. Zolotorev for useful discussions, and R. W. Falcone and S. Freedman for continued support. We would also like to thank W. Gawlik for comments on the manuscript. This work has been supported by NSF Grant No. PHY-9877046 and an REU supplement to NSF Grant No. PHY-9733479.

References

1. N.B. Delone, V.P. Krainov, *Nonlinear Optics of Atomic Gases*, (Wiley, New York, 1988).

2. D.C. Hanna, M.A. Yuratich, and D. Cotter, *Nonlinear Optics of Free Atoms and Molecules* (Springer-Verlag, Berlin, 1979).

3. R.W. Boyd, *Nonlinear Optics*, (Academic Press, San Diego, 1992).

4. Y.R. Shen, *The Principles of Nonlinear Optics*, (Wiley, New York, 1984).

5. R. H. Dicke, Phys. Rev. **93**, 99 (1954)

6. U. Domiaty, D. Gruber, L. Windholz, S.G. Dinev, M. Allegrini, G. De Filippo, F. Fuso, and R.-H.Rinkleff, Appl. Phys. B **59**, 525 (1994).

7. T. Stacewicz, N.A. Gorbunov, and P. Kozlowski, Appl. Phys. B, **66**, 461 (1998).

8. T. Stacewicz and P. Kozlowski, Appl. Phys. B, **65**, 69 (1997).

9. A. Dreischuh, V. Kamenov, S. Dinev, U. Reiter-Domiaty, D. Gruber, and L. Windholz, J. Opt. Soc. Am. B **15**, 34 (1998).

10. A. Dreischuh, U. Reiter-Domiaty, D. Gruber, L. Windholz, and S. Dinev, Appl. Phys. B **66**, 175 (1998).

11. M. Bashkansky, P. Battle, R. Mahon, and J. Reintjes, Opt. Commun. **120**, 189 (1995).

12. X. Han, Z. Lü, and Z. Ma, Opt. Commun. **67**, 383 (1988).

13. D.I. Chekhov, D.V. Gaidarenko, and A.G. Leonov, Opt. Commun., **105**, 209 (1994).

14. G. De Filippo, S. Guldberg-Kjaer, S. Milosevic, and J.O.P. Pedersen, Opt. Commun. **144**, 315 (1997).

15. W. Chalupczak, W. Gawlik, and J. Zachorowski, Phys. Rev. A, **49** 49 (1994).

16. W. Chalupczak, W. Gawlik, and J. Zachorowski, Optics Comm., **99** 49 (1993).

17. J.F. Valley, G. Khitrova, H.M. Gibbs, J.W. Grantham, and X. Jiajin, Phys. Rev. Lett. **64**, 2362 (1990).

18. A.S. Zibrov, L. Hollberg, M.D. Lukin, M.O. Scully, and V.L. Velichansky, in *Laser Spectroscopy* edited by R. Blatt, J. Eschner, D. Leibfried, and F. Schmidt-Kaler, (World Scientific, Singapore, 1999) p.362-3.

19. D. F. Kimball, to be published.

20. D.F. Kimball, D. Clyde, D. Budker, D. DeMille, S.J. Freedman, S. Rochester, J.E. Stalnaker, and M. Zolotorev, Phys. Rev. A **60**, 1103 (1999).

21. D.F. Kimball, Undergraduate Thesis, University of California at Berkeley (1998), available in electronic form at http://phylabs.berkeley.edu/budker.

22. *Handbook of Physical Quantities*, edited by I.S. Grigoriev and E.Z. Meilikhov (CRC Press, Boca Raton, FL, 1997).

23. C.J. Bowers, D. Budker, E.D. Commins, D. DeMille, S.J. Freedman, A.-T. Nguyen, S.-Q. Shang, and M. Zolotorev, Phys. Rev. A **53**, 3103 (1996).

24. M.S. Malcuit, D.J. Gauthier, and R.W. Boyd, Phys. Rev. Lett. **55**, 1086 (1985).

25. R.W. Boyd, M.S. Malcuit, and D.J. Gauthier, Phys. Rev. A **35**, 1648 (1987).

26. Y. Shevy, S. Hochman, M. Rosenbluh, Opt. Lett. **13**, 215 (1988).

27. W.R. Garrett, Phys. Rev. Lett. **70**, 4059 (1993).

28. W.R. Garrett, M.A. Moore, R.C. Hart, J.E. Wray, I Datskou, M.G. Payne, and R. Wunderlich, Phys. Rev. A **45**, 6687 (1992).

29. Estimates indicate that, in our case, the real part of the index of refraction for any wavelength differs from one by less than $\sim 10^{-2}$. Therefore, radical changes in wave vector direction are impossible.

30. D. DeMille, Phys. Rev. Lett. **74**, 4165 (1995).

31. D. Budker, *WEIN-98 Conference Proceedings* edited by C. Hoffman and P. Herzeg (World Scientific, River Edge, NJ, 1999).

32. M.-A. Bouchiat and C. Bouchiat, Rep. Prog. Phys. **60**, 1351 (1997).

33. C.J. Bowers, D. Budker, S.J. Freedman, G. Gwinner, J.E. Stalnaker, and D. DeMille, Phys. Rev. A **59**, 3513 (1999).

34. J.E. Stalnaker, Undergraduate Thesis, University of California at Berkeley (1998), available in electronic form at http://phylabs.berkeley.edu/budker.

35. I.B. Khriplovich, *Parity Nonconservation in Atomic Phenomena* (Gordon and Breach, Philadelphia, 1991).

Table I: Summary of observed emissions.

EMISSION λ (nm)	**DIRECTION**	**COLLIMATED**	**CONICAL**
649	Forward	X	
	Backward	X	
680	Forward	X	X
	Backward	X	
611	Forward	X	X
556	Forward		X

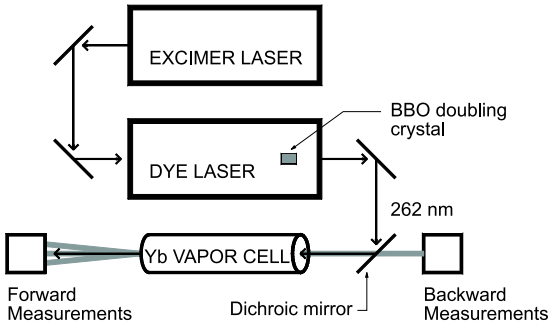

Fig. 1. Schematic diagram of experimental set-up.

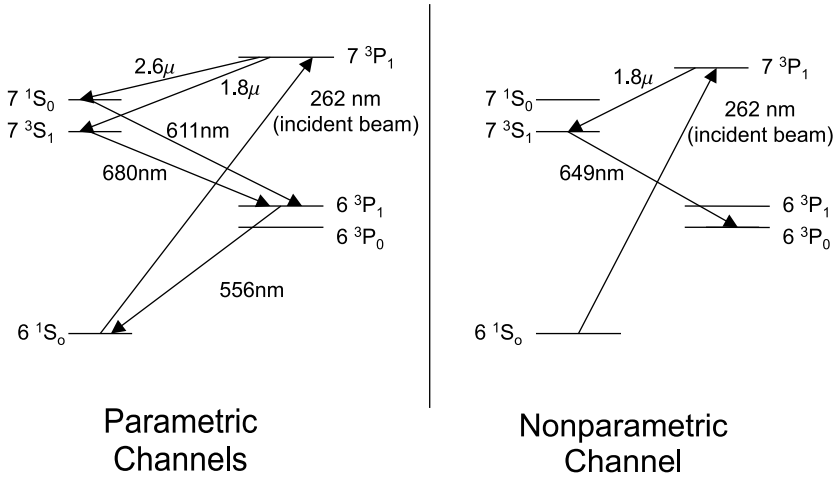

Fig. 2. Primary "channels" observed when the pump beam is tuned near the one-photon Yb 6 $^1S_0 \rightarrow 7\ ^3P_1$ transition. Transitions between the 6 $^3P_0$ state and the ground state are strictly forbidden because the two states have zero angular momentum.

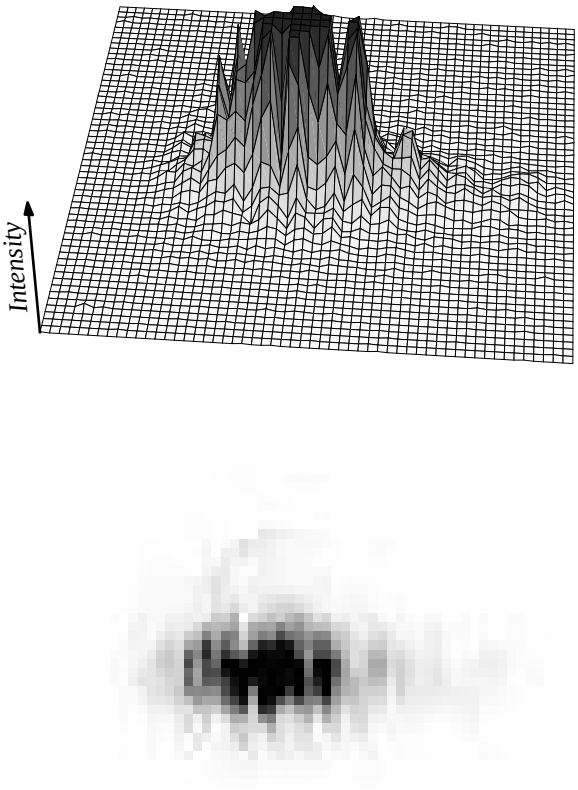

Fig. 3. Plots of spatial intensity distribution of 649 nm emission in the forward direction (single pulse) measured with a CCD camera: both three-dimensional and grayscale plots of intensity vs. position are shown. Cell temperature is ≈1150 K, buffer gas (Ne) pressure is ∼10 Torr, and incident 262 nm light is detuned to the high frequency side of resonance by ≈ 5 GHz (a fraction of the laser linewidth). The spatial intensity distribution of 649 nm emission is qualitatively similar throughout the tuning range of 262 nm light where such emission is observed.

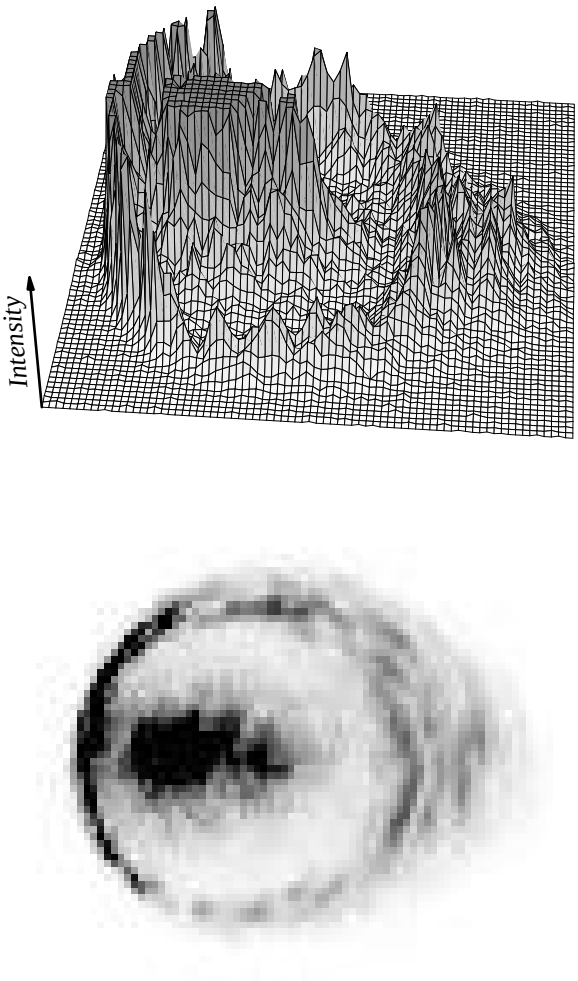

Fig. 4. Plots of spatial intensity distribution of 680 nm emission in the forward direction (single pulse) measured with a CCD camera; same experimental conditions as in Fig. 3. Note both CE and spatially-resolved collimated emission inside the cone. The choice of optical filters was a compromise between reduced saturation of the CCD and the ability to see all relevant features of the emission.

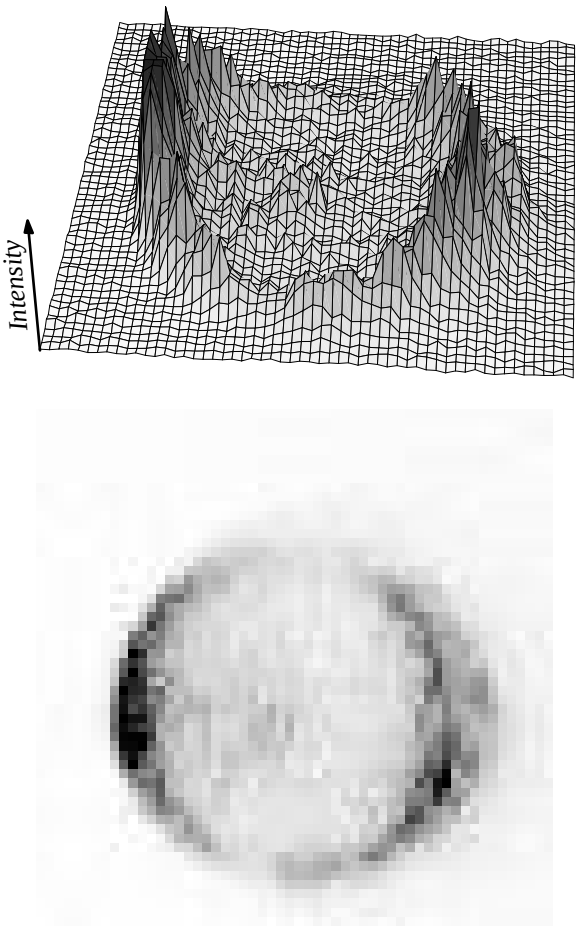

Fig. 5. Plots of spatial intensity distribution in the forward direction (single pulse) of 611 nm emission measured with a CCD camera; same experimental conditions as in Fig. 3.

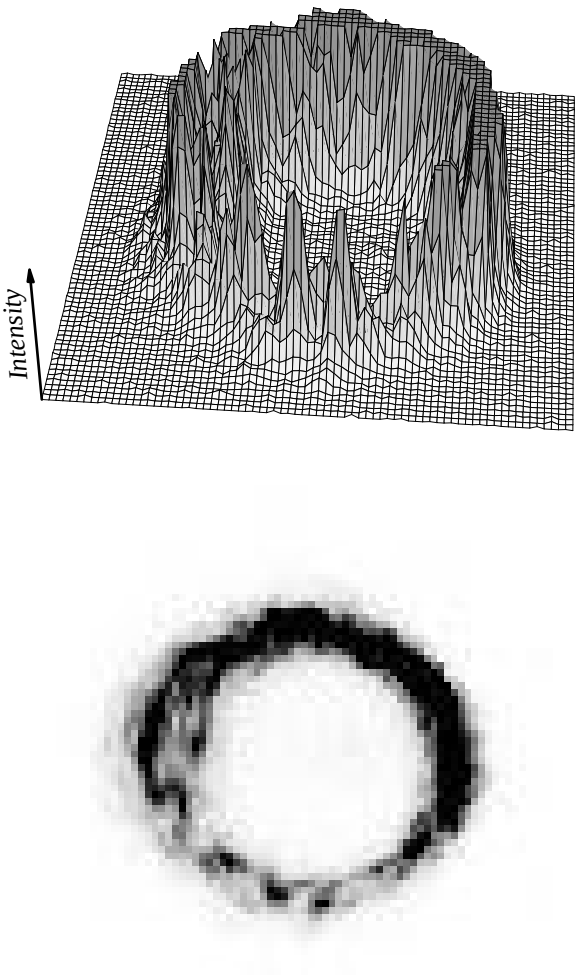

Fig. 6. Plots of spatial intensity distribution in the forward direction (single pulse) of 556 nm emission measured with a CCD camera; same experimental conditions as in Fig. 3.

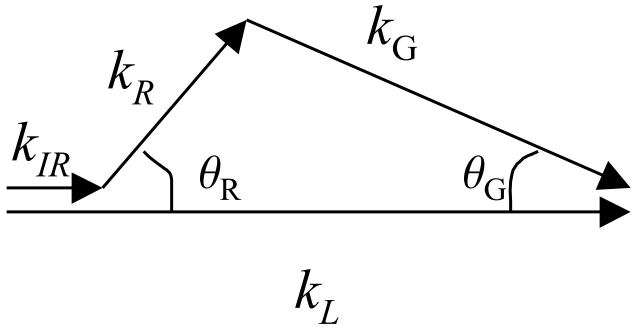

Fig. 7. Illustration of phase matching conditions for parametric four-wave mixing (4WM). Since ω_G is nearly resonant with a strong transition coupling to the atomic ground state, the susceptibility for ω_G can be relatively large. Therefore, $|\vec{k}_G|+|\vec{k}_R|+|\vec{k}_{IR}|$ can be greater than $|\vec{k}_L|$. In order to satisfy momentum conservation, light must be emitted off-axis, causing CE at multiple wavelengths. This illustration assumes that IR light, possibly originating from stimulated Raman scattering (SRS), propagates collinearly with the excitation beam. Fields at frequencies ω_G and ω_R can build up from noise via parametric amplification.

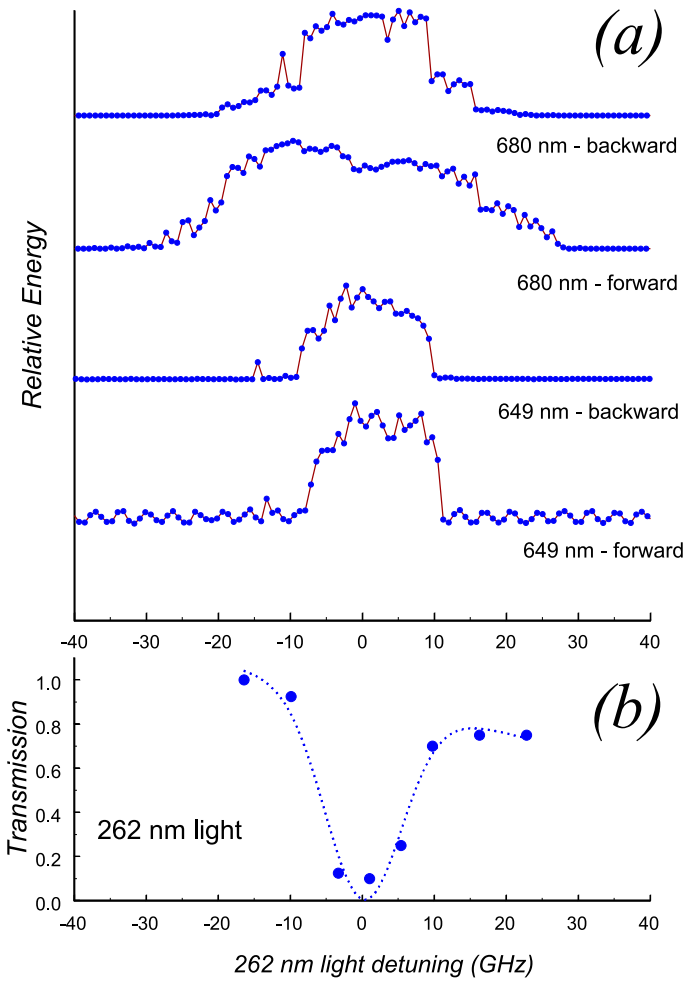

Fig. 8. Dependence of nonlinear emissions observed in both the forward and backward on 262 nm light detuning. (a) Relative energy of emitted radiation with respect to incident 262 nm light detuning. Cell temperature is ≈1100 K, Ne pressure is ≈3 Torr; (b) Intensity of low power 262 nm light (where no nonlinear optical effects are observed) after passing through the vapor cell. Overall slope is caused by approximately linear decrease in initial laser intensity as a function of detuning.

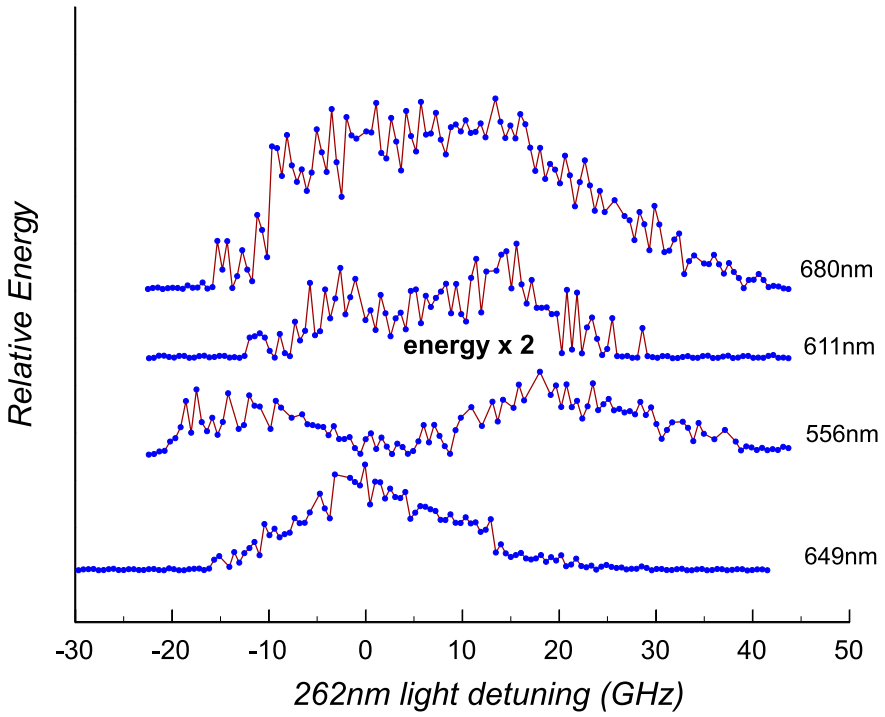

Fig. 9. Relative energy with respect to detuning of incident 262 nm light of each visible wavelength emitted in the forward direction. Cell temperature ≈1150 K, Ne pressure ≈10 Torr. Relative energy of 611 nm emission is multiplied by two with respect to energies of other wavelengths, since emitted intensity at this wavelength is smaller than for the other wavelengths. Note that the 556 nm emission, which can be produced only by parametric 4WM, has reduced intensity near the 262 nm resonance, whereas the 649 nm emission, which is produced purely through nonparametric processes has maximum intensity near the 262 nm resonance.

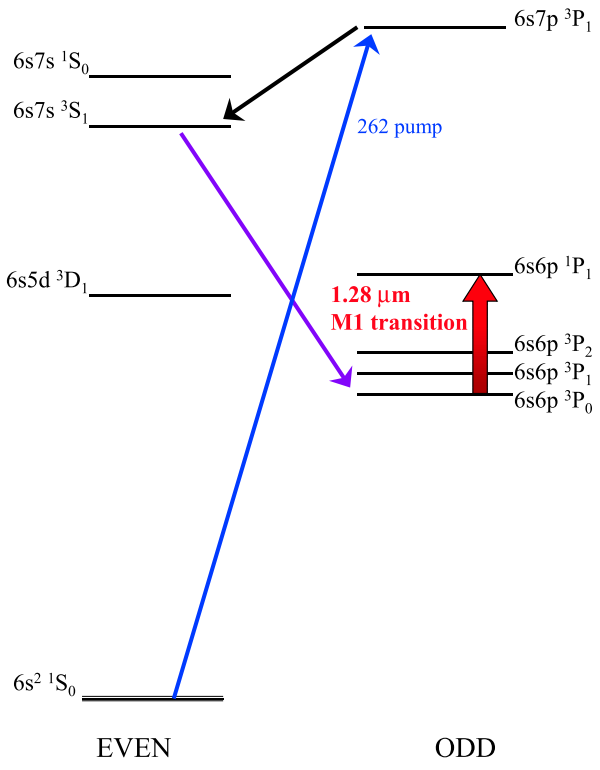

Fig. 10. Low-lying Yb energy levels and relevant transitions for measurement of PNC-induced optical rotation.